



**Interdigitated microelectronic bandage augments
hemostasis and clot formation at low applied voltage in
vitro and in vivo**

Journal:	<i>Lab on a Chip</i>
Manuscript ID	LC-ART-06-2018-000573.R1
Article Type:	Paper
Date Submitted by the Author:	31-Jul-2018
Complete List of Authors:	<p>Hardy, Elaissa; Georgia Institute of Technology Wallace H Coulter Department of Biomedical Engineering; Children's Healthcare of Atlanta Inc, Aflac Cancer Center and Blood Disorders ; Emory University School of Medicine, Department of Pediatrics</p> <p>Wang, Yannan; Georgia Institute of Technology Wallace H Coulter Department of Biomedical Engineering</p> <p>Iyer, Sanathan; Georgia Institute of Technology Wallace H Coulter Department of Biomedical Engineering</p> <p>Mannino, Robert; Georgia Institute of Technology Wallace H Coulter Department of Biomedical Engineering; Children's Healthcare of Atlanta Inc, Aflac Cancer Center and Blood Disorders; Emory University School of Medicine, Department of Pediatrics</p> <p>Sakurai, Yumiko; Georgia Institute of Technology Wallace H Coulter Department of Biomedical Engineering; Children's Healthcare of Atlanta Inc, Aflac Cancer Center and Blood Disorders; Emory University School of Medicine, Department of Pediatrics</p> <p>Barker, Thomas; University of Virginia, Department of Biomedical Engineering</p> <p>Chi, Taiyun; Georgia Institute of Technology College of Engineering, School of Electrical and Computer Engineering</p> <p>Youn, Yeojoon; Georgia Institute of Technology College of Engineering, School of Electrical and Computer Engineering</p> <p>Wang, Hua; Georgia Institute of Technology, Electrical and Computer Engineering</p> <p>Brown, Ashley; North Carolina State University College of Engineering, Biomedical Engineering; North Carolina State University Comparative Medicine Institute</p> <p>Lam, Wilbur; Aflac Cancer Center and Blood Disorders Service, Department of Pediatrics, Emory University; Georgia Institute of Technology, The Wallace H. Coulter Department of Biomedical Engineering</p>

1 Interdigitated microelectronic bandage augments hemostasis and clot formation at low applied
2 voltage *in vitro* and *in vivo*

3
4 Elaissa T. Hardy¹⁻³, Yannan J. Wang¹, Sanathan Iyer¹, Robert G. Mannino¹⁻³, Yumiko Sakurai¹⁻³,
5 Thomas H. Barker⁴, Taiyun Chi⁵, Yeojoon Youn⁵, Hua Wang⁵, Ashley C. Brown^{6,7}, and Wilbur
6 A. Lam*¹⁻³

7
8 *corresponding author

9 ¹Wallace H. Coulter Department of Biomedical Engineering, Georgia Institute of Technology
10 and Emory University, Atlanta, Georgia, USA ²Aflac Cancer Center and Blood Disorders
11 Service of Children's Healthcare of Atlanta, Atlanta, Georgia, USA ³Department of Pediatrics,
12 Emory University School of Medicine, Atlanta, Georgia, USA ⁴Department of Biomedical
13 Engineering, University of Virginia, Charlottesville, Virginia, USA ⁵School of Electrical and
14 Computer Engineering, Georgia Institute of Technology, Atlanta Georgia, USA ⁶Joint
15 Department of Biomedical Engineering, North Carolina State University and University of North
16 Carolina at Chapel Hill, Raleigh, North Carolina, USA ⁷Comparative Medicine Institute, North
17 Carolina State University, Raleigh, NC, USA

18
19

20 Corresponding Author:

21 Wilbur A. Lam, MD, PhD

22 Emory University School of Medicine

23 2015 Uppergate Drive NE #448

24 Atlanta, GA 30322

25 404-727-7473

26 wilbur.lam@emory.edu

27

28 ABSTRACT

29 Hemorrhage or uncontrolled bleeding can arise either due to a medical condition or from
30 a traumatic injury and are typically controlled with the application of a hemostatic agent.
31 Hemostatic agents are currently derived from animal or human products, which carry risks of
32 blood borne infections and immune dysregulation. Therefore, the need exists for novel
33 biomedical therapies not derived from animal or human products to achieve hemostasis.
34 Accordingly, we created an interdigitated microelectronic bandage that applies low voltage
35 electrical stimulation to an injury site, resulting in faster clot formation without excessive
36 heating, accelerated fibrin formation, and hemostasis overall. Our interdigitated microelectronic
37 bandage found fibrin formed 1.5x faster *in vitro*. *In vivo*, total cessation of bleeding was 2.5x
38 faster, resulting in 2x less blood loss. Electricity has been used in medical applications such as
39 defibrillation, cauterization, and electrosurgery, but scant research has focused on hemostasis.
40 Here we report a novel surface treatment using interdigitated microelectronic device that creates
41 rapid hemostasis in both *in vitro* and *in vivo* bleeding models with low applied voltages,
42 representing a new and novel class of hemostatic agents that are electrically-based.

43

44

45 INTRODUCTION

46 As hemorrhage due to trauma, surgery, and bleeding disorders remains a major cause of
47 mortality and morbidity, a need exists for novel therapies to achieve hemostasis. Current
48 hemostatic agents are blood products that increase the effective concentration of blood
49 coagulation proteins and are derived from animal or human products, which carry risks of blood
50 borne infections and immune dysregulation^{1,2,3,4,5}. Topical agents, such as tissue adhesives
51 have gained popularity in closing small simple lacerations and surgical incisions^{6,7}. Tissue
52 adhesives are hemostatic and form an occlusive dressing that can create an antimicrobial barrier
53 and moist wound environment⁸. However, they are not recommended for mucosal surfaces and
54 lacerations that have wound tension⁹. Alternatively, electricity has historically been used in a
55 variety of medical applications such as defibrillation, cauterization, and electrosurgery to achieve
56 hemostasis^{8,10,11} but result in creating unwanted damage to the surrounding tissue and require
57 specialized equipment^{12,13}.

58 Inherent with the current hemostatic therapies listed above is the need for specialized
59 equipment or temperature-controlled storage, which may not be readily available and are
60 primarily used by trained professionals. Additionally, hemorrhage due to trauma typically occur
61 away from the hospital where medical resources are limited. Therefore, a need exists for a novel
62 biomedical solution for non-compressible hemorrhage that decreases the chance for secondary
63 infections and healing complications, is comprised of a simple device requiring no specialized
64 equipment, training or temperature-controlled storage, and is readily available in any resource
65 setting.

66 Herein, we present results of our novel interdigitated microelectronic device incorporated
67 into a simple surface treatment band aid. The microelectronic device uses low voltages (1-

68 60Volts) to create rapid hemostasis in both *in vitro* and *in vivo* bleeding models. Our *in vitro*
69 bleeding models used human whole blood in direct contact with the stimulated electrical field,
70 finding faster clot formation without excessive heating of the blood and avoided thermal tissue
71 destruction. Further investigation towards the mechanism of blood coagulation found that the
72 low voltage electrical fields accelerate the direct conversion of fibrinogen into fibrin and hence
73 hemostasis overall. To our knowledge, this research is the first focusing on low voltage with the
74 intent to avoid tissue destruction. This application of low voltage-surface treatment to sites of
75 vascular injury represents an entirely new and novel class of hemostatic agents that are
76 electrically-based (wherein are free from the infectious risks and immune effects that encumber
77 current human or animal-derived agents) and will have significant implications for experimental
78 and clinical hematology.

79

80 EXPERIMENTAL

81 Shadow Mask and Metallized Microelectronic Device

82 Shadow masks were cut from stainless steel using a CO₂ laser in an interdigitated pattern with
83 0.25mm thick fingers, 0.75mm apart, spanning 1cm. The shadow masks were adhered to 20 mm
84 x 20 mm glass coverslips and metal was evaporated onto the glass coverslip substrate using an
85 electron beam evaporator. 20nm of Titanium was deposited as the adhesion metal, followed by
86 200nm of Gold. Thicknesses were confirmed with a surface profilometer.

87

88 PDMS Devices

89 Two polydimethylsiloxane (PDMS) microfluidic devices were created: T-shaped device (Figure
90 2a) and single channel devices (Figure 3a) using a DIY-microfluidic process¹⁴ (Sylgard 184

91 Silicone Elastomer Kit from Dow Corning, Midland, MI). 1.3mm square wire was adhered to the
92 bottom of a petri dish and 10:1 (base material: curing agent) PDMS was poured over the mold
93 and cured overnight in 60 °C oven. For the T-shaped microfluidic devices, separate pieces of
94 PDMS approximately 0.5mm thick, were cured and punched with a 4mm biopsy punch to create
95 the top well. PDMS was spun into thin layers and used to bond the two pieces together, and the
96 devices were cured overnight in a 60 °C oven before use. For the single channel devices, the
97 channels were cut to be the same length as the 20 mm x 20 mm glass coverslip device and
98 bonded to the glass coverslips by spreading a thin layer of PDMS to effectively glue the two
99 pieces together. The channels were cured in a 60 °C oven overnight before use.

100

101 Live Subject – Human Blood Treatment

102 All experiments were performed in compliance with the relevant laws and Georgia Institute of
103 Technology, USA guidelines. Human blood was collected according to Georgia Institute of
104 Technology's IRB-approved protocols per the Declaration of Helsinki. Informed consent was
105 obtained from all human subjects.

106 0.2mL citrate was added to 2.7mL of whole blood. Before use, 990 μ L of blood was recalcified
107 using 10 μ L 0.1M CaCl₂. 25 μ L human fibrinogen conjugate with fluorescent dye Alexa Fluor
108 488 (purchased from Life Technologies) was added to the 1000 μ L of recalcified blood in order
109 to visualize fibrin formation.

110

111 Application of Electric Field

112 An Agilent E3649A DC power supply was used to generate the applied electric field where
113 voltage was sourced. DC power was selected to emulate a battery.

114

115 Temperature Measurements

116 A thermocouple probe was placed into the microfluidic channel to measure the change in
117 temperature during *in vitro* experiments. Temperature was recorded on a Fluke 179 TRUE RMS
118 Multimeter.

119

120 Live Subject - Animal injury model

121 All experiments were performed in compliance with the relevant laws and Georgia Institute of
122 Technology, USA guidelines. All protocols are approved by the Georgia Institute of Technology
123 IACUC prior to implementation.

124 Adult Sprague-Dawley male rats (200-250g) are anesthetized with 5% isoflurane. Following
125 anesthesia, an incision is made on the right hind limb to expose the femoral vessels. A portion of
126 the femoral vein is isolated from the surrounding connective tissue by placing a small piece of
127 foil between the vessel and the underlying tissue. The cavity is then irrigated with 0.9%
128 irrigation fluid at 37 °C. Following a 5 minute equilibration time, injury is induced to the right
129 femoral vein by piercing the vein with a 22gauge needle. Our experimental microelectronic
130 wound dressing is then placed directly over the injury and electrical pulse is applied for 10 secs.
131 Control groups include wound dressings with no electrical pulse and no treatment. Six animals
132 were analyzed at 9V and three animals for 3V and 6V, each. A gauze is also lightly placed below
133 the injury site to collect blood, allowing for measurement of total blood loss without disturbing
134 the injury site. Gauze is changed every 10 secs for the first 30 sec following injury and then
135 every 30 secs until bleeding ceases. Bleeding time is defined as the time required for bleeding to
136 cease for a minimum of 10 secs. Following cessation of bleeding, animals are euthanized with

137 carbon dioxide and organs separated, fixed with 10% formalin, paraffin embedded and 5 μ m
138 sections are produced using a Microm 355H Microtome (Thermo Scientific) and MSB staining
139 was performed to visualize fibrin formation.

140

141 Supplementary Figure 1: PDMS chamber: A polydimethylsiloxane (PDMS) chamber with
142 embedded metallic wires (Platinum wire with a diameter of 0.1mm) was created to hold 150 μ L
143 of liquid. The metallic wires were connected to an Agilent E3649A variable power supply and a
144 constant voltage was applied to the chamber for up to 5 minutes. A Fluke 179 multimeter
145 monitored the temperature with a thermocouple lead inserted into the liquid in the chamber.
146 Experiments were conducted using whole human blood anti-coagulated with acid citrate dextrose
147 and with isolated platelet rich plasma (PRP), platelet poor plasma (PPP), and washed platelets.

148

149 Supplementary Figure 2: Human whole blood was treated as described previously in Blood
150 Treatment. To visualize the platelets, antibodies, Integrin alpha 2b/CD41 Antibody (NB100-
151 2614) M148 purchased from Novus Biologicals and plasma membrane stain (CellMask Deep
152 Red), fluorescently-tagged secondary antibodies goat anti-mouse IgG (A-11004) purchased from
153 Thermo Fisher Scientific were used.

154

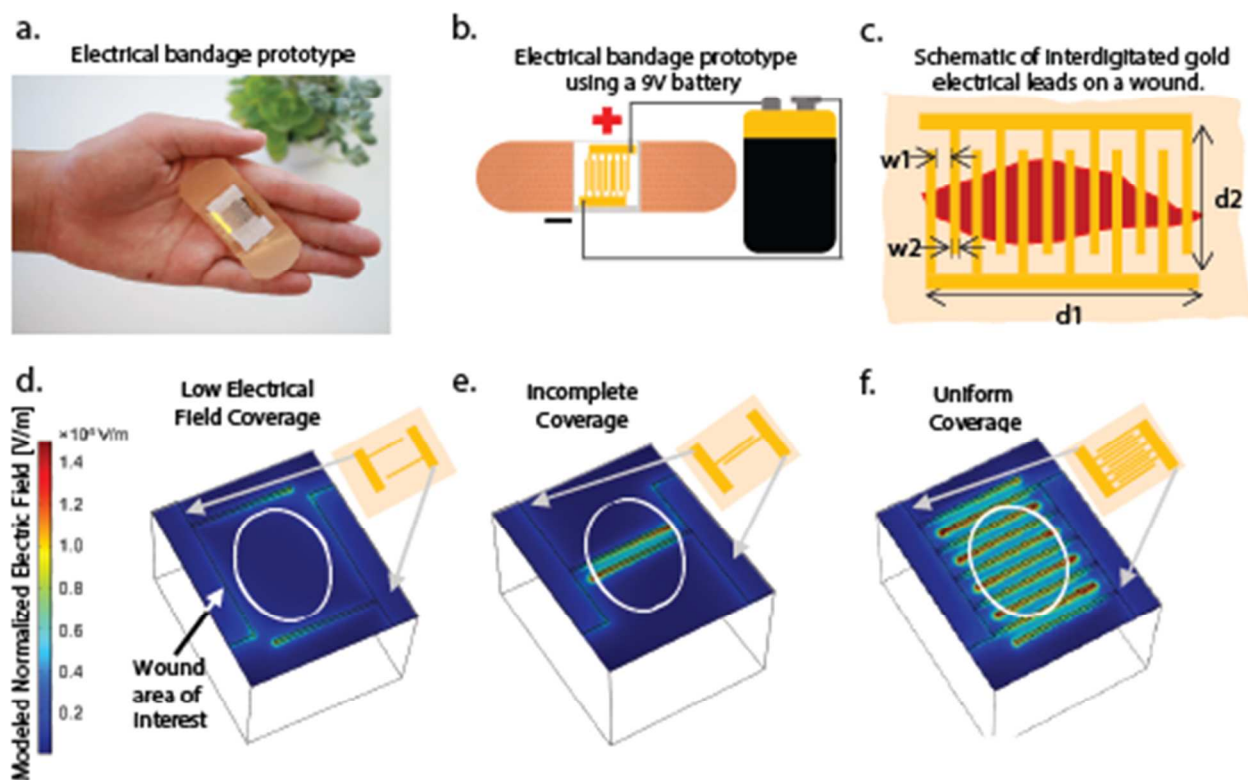
155 Supplementary Figure 3: T-shaped devices were used as described previously in PDMS Devices.
156 Experiments followed Blood Treatment and Application of Electric Field also described
157 previously. Standard compression was applied to the top well (the injury site) with a 200-g scale
158 weight.

159

160 RESULTS & DISCUSSION

161 Design, characterization, and optimization of microelectronic devices

162 This research investigated the application of low voltage (1-60V) to augment hemostasis
 163 and could this concept be leveraged and incorporated into a bandage or wound dressing. Figure
 164 1a and b show our microelectronic bandage prototype with the interdigitated electrodes “fingers”
 165 with the anode and cathode bus bars connected to a 9V battery. The 9V battery allows for
 166 portability, simple use, and provides direct current (DC), an important feature of the system that
 167 will be discussed throughout.



168

169 **Figure 1** – a. Electrical bandage prototype with gold interdigitated electrical leads. b. Representative cartoon of the
 170 electrical bandage prototype using a 9V battery. The 9V battery was selected for portability and the ability to
 171 provide direct current to the bandage. c. Schematic cartoon of the electrical bandage on a wound with dimensions of
 172 interest being d_1 , the length of the device, and d_2 , the height of the device. COMSOL modeling was used to
 173 determine the optimal configuration of the interdigitated fingers d. Two leads spread far apart with low electrical
 174 field coverage. e. Two leads next to each other resulting in incomplete electrical field coverage, and f. Interdigitated
 175 leads showing uniform coverage throughout the wound area of interest.

176

177 The use of interdigitated electrode arrays was introduced in the late 1990's as
178 biochemical sensors, where the alternating positive and negative electrodes created a uniform
179 electric field, allowing for improved sensitivity measurements¹⁵. Interdigitated electrodes have
180 continued to be popular as bioelectrical sensors¹⁶ and electrical sensors¹⁷ because of their
181 uniformity and simple fabrication. Additionally, the size of the array can be expanded or
182 decreased while maintaining the uniform electric field, providing flexibility in our design and
183 incorporation into a wound dressing. Initial research focused on the size of the array, Figure 1c
184 shows the dimensions of interest, specifically the length (d1) and width (d2) as related to the size
185 of a wound. Using COMSOL Multiphysics software (Figure 1d, e and f), the normalized
186 electrical field [V/m] was modeled to demonstrate the electrical potential of our interdigitated
187 microelectronic device with various finger spacing. Equal field amplitude (uniform coverage)
188 over the entire wound dressing active area, was achieved in Figure 1f using multi-fingers and
189 small spacing as compared to large finger spacing (Figure 1d) or a single set of fingers (Figure
190 1e). The uniform electrical field coverage correlates experimentally with uniform polymer fibrin
191 formation spreading throughout the device (not shown here). Simulations also show that the
192 geometry of the device matters: working most effectively when the interdigitated fingers were
193 placed on the edges of the wound and covered the entire wound, as placement is diagrammed in
194 Figure 1c. For this *in vitro* work, we created circular wounds with diameters between 0.4 – 1 cm
195 with $d1 = 1$ cm and $d2 = 1$ cm.

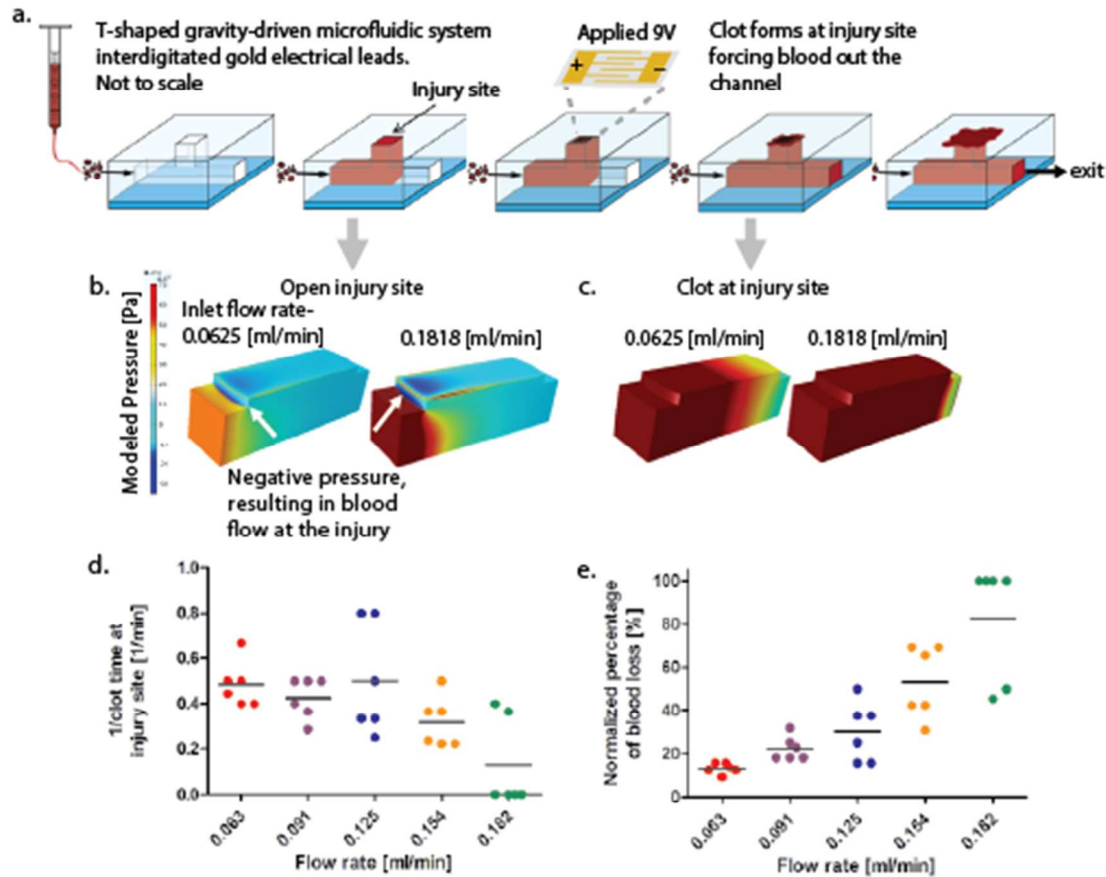
196 Also, of interest is the spacing between fingers (w1) and diameter of the fingers (w2)
197 (Figure 1c), which were set as $w1 = 0.75$ mm and $w2 = 0.25$ mm. These values were also used
198 in the above COMSOL models. As stated in Gerwen¹⁵, approximately 95% of the current created
199 will have a penetration distance equal to the finger spacing (w1) plus the finger diameter (w2).

200 Therefore, in our design, 95% of the current created will have a penetration distance of 1 mm.
201 As will be discussed with our animal injury models, rat femoral arteries have a diameter of ~ 0.89
202 mm^{27} , therefore our devices have sufficient penetration distance for the *in vivo* experiments. It
203 should be noted that generated current will be affected by the resistance of blood and nearby by
204 tissue following Ohm's law, this will be discussed in more detail.

205 We next focused on understanding the experimental parameter space in regards to the
206 blood product (washed platelets, platelet rich plasma, platelet poor plasma, or whole blood), and
207 the temperature and current limits when applying 1-60V. Below 15V both platelets and plasma
208 are needed for rapid electrical-activated clotting to occur (Supplementary Figure 1a) therefore,
209 we focused solely on whole blood (plasma, red blood cells, white blood cells, and platelets).
210 When applying an electric field, the heat generated and physiological effects generated by
211 current are important. Temperature (i.e. heat generated effects) will increase with increasing
212 voltage and thermal tissue damages caused by temperatures below $45\text{ }^{\circ}\text{C}$ are considered
213 reversible¹⁸, which correspond here to voltages less than 30V for anti-coagulated whole blood,
214 shown in Supplemental Figure 1b. Additionally, we measured the peak current in the devices at
215 various applied voltages as shown in Supplemental Figure 1c. From Ohm's law¹⁹ (and references
216 therein), current is equal to voltage divided by resistance, and is the amount of electrical charges
217 flowing per second, measured in amperes (A). Most current-related effects result from heating of
218 tissues, stimulations of muscles and nerves, and approximately 0.03A of current can cause
219 respiratory paralysis²⁰. Our results found that applied voltages below 15V, resulted in currents
220 less than 0.03A for anti-coagulated whole blood, therefore we will further limit our parameter
221 space to voltages less than 15V. Lastly, because our prototype microelectronic bandages are
222 designed for direct contact with the wound and surface tissue, we placed the prototype

223 microelectronic bandages on simulated tissue (pre-purchased bovine muscle) and varying
224 voltages were applied to the bandage for 2 minutes to visually see the impact. Voltages between
225 10-30V had visible black charring on the simulated tissue wound (Supplemental Figure 1d),
226 whereas at 9V there was no visible damage to the simulated tissue wounds (Supplemental Figure
227 1e), therefore experiments were further limited to voltages below 9V.

228 To test the initial efficacy microelectronic field devices to mediate hemostasis, an easily
229 replicable yet physiologic bleeding model²¹ was needed. To that end, we developed an *in vitro*
230 bleeding model using a gravity-driven microfluidic system (Figure 2a – not to scale) to mimic an
231 *in vivo* rat femoral vessel traumatic injury model. Based on the literature, typical reported rat
232 femoral vessel blood flow rates range from 0.2ml/min to 7.1ml/min^{22,23}. Blood flow was
233 perfused in a gravity-driven manner, as opposed to a conventional pump-driven system, into a
234 simulated wound and to observe whether application of electrical stimulation would augment
235 hemostasis and therefore decrease the overall time required for bleeding to cease. With the
236 gravity-driven system, the flow rate can be increased by adjusting the height of the syringe,
237 which will increase or decrease the flow rates. Using COMSOL modeling, we modeled the
238 injury site with our minimum and maximum flow rates, specifically looking at the pressure with
239 the injury site open (Figure 2b) and closed to mimic a clot (Figure 2c). With the injury site open,
240 there are distinct regions of negative pressure, resulting in blood flow up into the injury site.
241 With the injury site closed (mimicking a clot), the pressure gradient remains nearly constant
242 indicating that the blood will flow out of the exit.



243

244 **Figure 2** – a. Cartoon schematic (not to scale) of a T-shaped gravity-driven microfluidic system with interdigitated
 245 gold electrical leads where blood flowed into the microfluidic, 9V was applied to the electrical field device, time
 246 was recorded for when a clot was formed at the injury site, forcing the remaining blood out of the channel. b.
 247 COMSOL modeling of the pressure in the channel at the injury site for 0.0625ml/min and 0.1818ml/min with an
 248 open injury site and c. with a closed injury site to mimic a clot. Focusing on the injury site, the results of various
 249 flow rates with 9V applied electrical field device are presented in d. 1/clot time and e. Normalized percentage of
 250 blood loss.

251

252

Re-calcified citrated human whole blood was perfused through the *in vitro* bleeding

253

model at various flow rates. The interdigitated microelectronic device, was placed on the

254

microfluidic injury site, allowing for direct contact with the whole blood with applied 9V. Time

255

was recorded from the point the blood entered the microfluidic until the time at which a clot

256

formed on the microelectronic device and the blood began to flow out of the channel. The 1/clot

257

time at the injury site results are presented in Figure 2d with an n=6 for all the flow rates. The

258

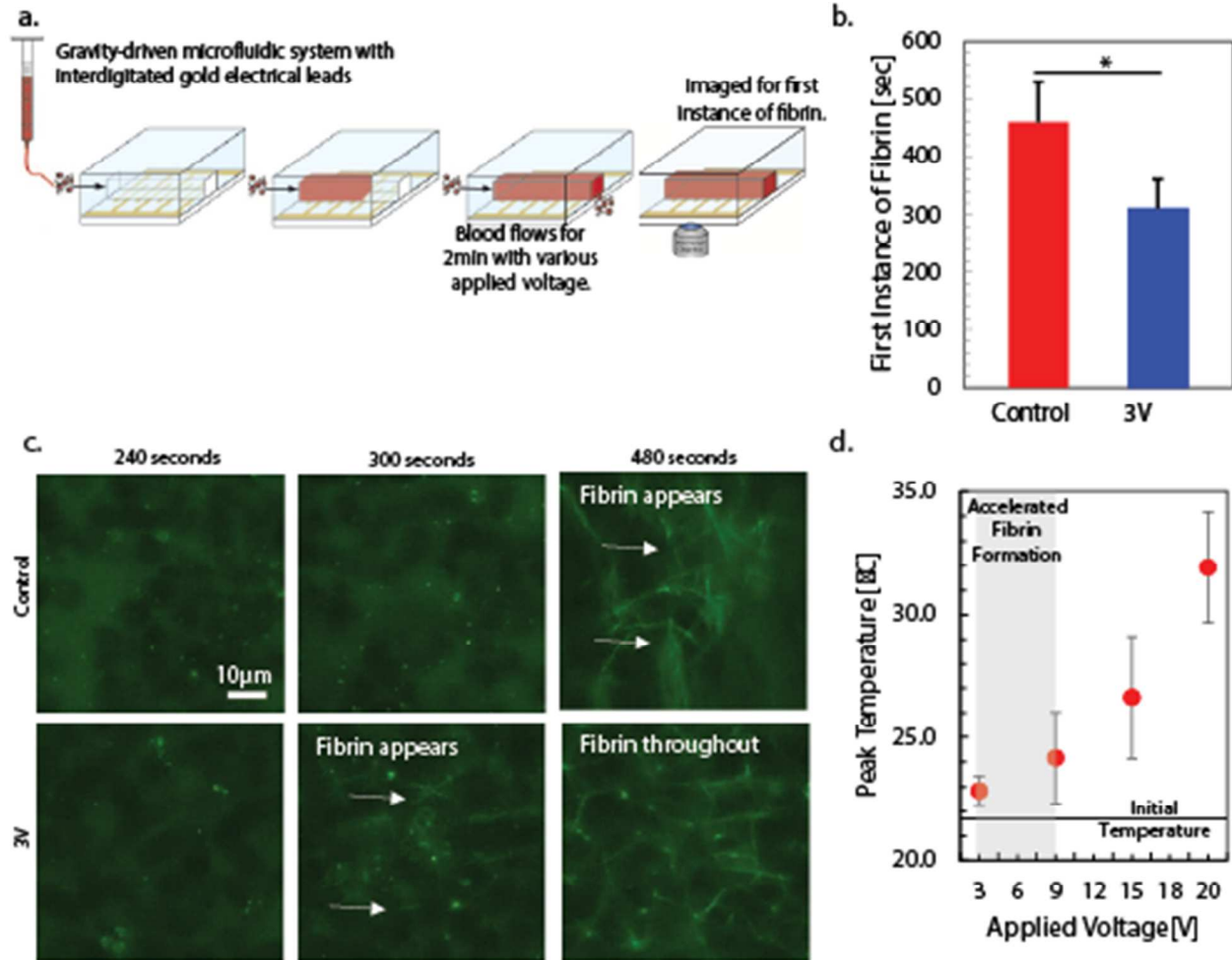
fastest time to form a clot occurred at 0.8[1/min] equal to 1 minute 15 seconds, whereas the

259 slowest time recorded was 0.2[1/min] equal to 4 minutes 30 seconds. This set of experiments is
260 plotted again as normalized percentage of blood loss (Figure 2e), where statistically significance
261 was found between all flow rates with a P-value less than 0.01 except between 0.091ml/min and
262 0.125ml/min. Additionally, we investigated the use of pressure on this device at the
263 0.063ml/min flow rate as shown in Supplemental Figure 3. The application of pressure was
264 achieved with the use of a 200 g scale weight²⁸ with and without the application of 9V. Using
265 the Mann-Whitney U test, we found that application of pressure alone led to much longer
266 clotting times than with the application of 9V alone ($p = 0.0079$) or application of 9V and
267 pressure ($p = 0.0079$). No statistical difference was detected in clotting time between application
268 of 9V and 9V with applied pressure ($p = 0.1746$). As such, the application of pressure does not
269 decrease clotting time nor further augment clot formation associated to applied voltage.
270 Therefore, we have developed an *in vitro* bleed model that incorporates our microelectronic
271 device and mediates hemostasis creating a novel biomedical solution for non-compressible
272 hemorrhage.

273 Natural blood coagulation is a complicated process that has been extensively studied²⁴.
274 The coagulation cascade includes various pathways and many reactions, but always concludes
275 with the enzyme thrombin converting fibrinogen into cross-linked fibrin fibers²⁵, where the fibrin
276 fibers form long strands of tough insoluble protein that are bound to platelets, creating a mesh
277 plug at the wound site. As such, we focused on discerning the underlying mechanism of fibrin
278 formation at the microscope level *in vitro*. To visual the first instance of fibrin formation, the
279 microfluidic bleeding model was redesign to be a simple PDMS channel placed on top of the
280 microelectronic device (Figure 3a). Re-calcified citrated human whole blood with added
281 fluorescently-tagged fibrinogen was perfused at physiologic flow conditions (0.063ml/min)

282 through the microfluidic channel. Voltage was applied for 2 minutes, followed by
283 epifluorescence microscopy to visualize the first instance of fibrin formation. Figure 3b shows a
284 comparison of fibrin formation when 3V was applied for 2 minutes as compared to a control
285 sample where no voltage was applied. Statistical significance was found between the control and
286 3V (n=32), therefore applied electric fields induce direct conversion of fibrinogen to fibrin and
287 rapid hemostasis. Of note, voltage less than 3V demonstrate this phenomenon albeit slower,
288 whereas voltages between 4-9V resulted in bubbles in the channel, therefore lysed blood cells,
289 and no visualization of fibrin. Figure 3c shows representative images of the fibrin formation at 4
290 minutes, where in both conditions (control and 3V) there is no presence of fibrin, at 5 minutes,
291 where the first instance of fibrin is found only in the 3V condition, and at 8 minutes, where both
292 conditions had fully formed fibrin throughout. Temperature was measured within the
293 microfluidic to determine if temperature increase was associated with faster fibrin formation.
294 Figure 3d displays the peak temperature measured during the 2-minute duration of applied
295 voltage, and the shaded region represents the time window in which accelerated fibrin formation
296 occurs in the *in vitro* devices. At 3V, the temperature remains below 24°C and up to 20V the
297 temperature remains below 35°C. The results show that while increased voltage is associated
298 with an increase in temperature, the temperature change is not physiologically significant in the
299 regime in which fibrin formation is accelerated and therefore we cannot attribute our findings to
300 just temperature change in our *in vitro* experiments. Additionally, we fluorescently labeled
301 platelets to investigate whether an increase in platelet aggregation or adhesion is associated with
302 applied voltage. We did not detect a significant change in platelet aggregation or adhesion or a
303 significant difference in the total number of platelets in the control versus 3V experiments
304 (shown in Supplementary Fig 2).

305



306

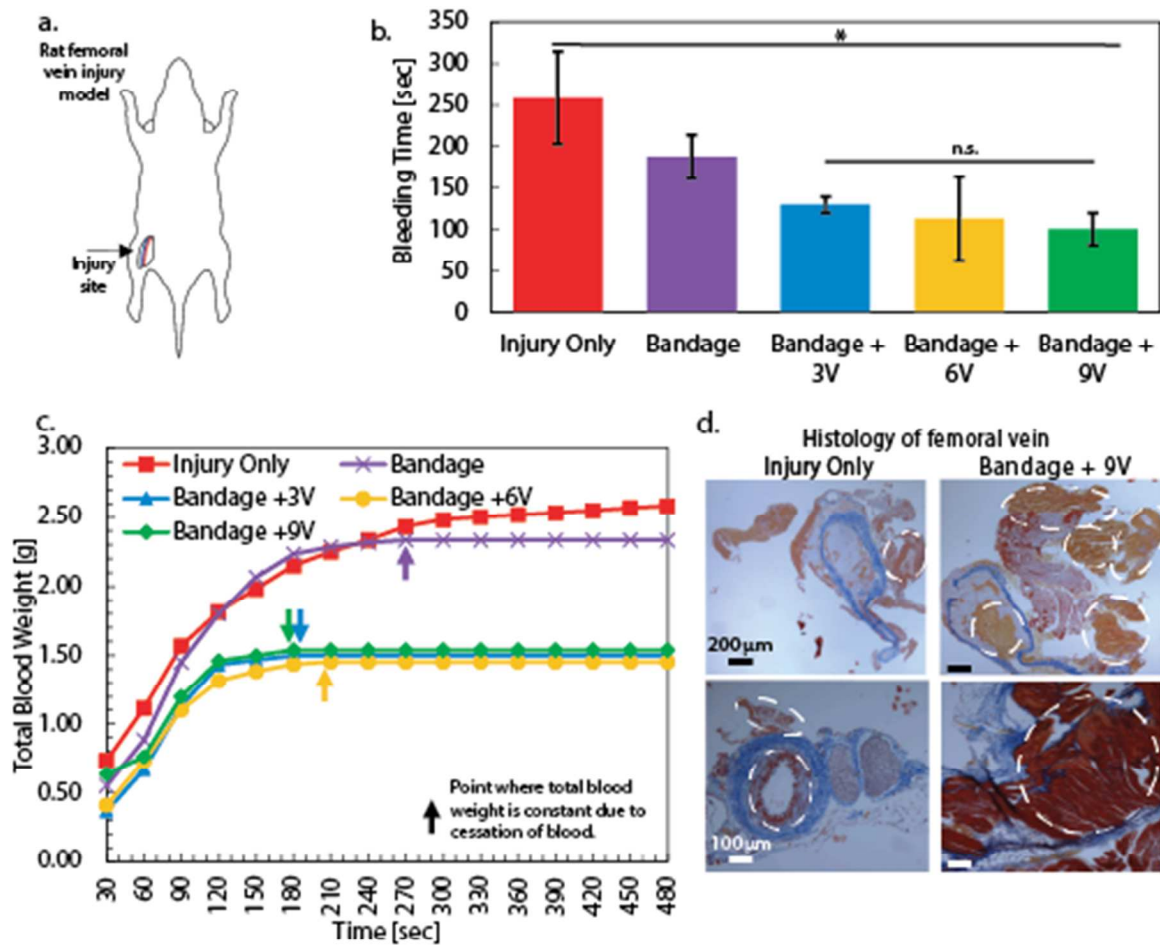
307 **Figure 3** – a. Cartoon schematic of a single channel gravity-driven microfluidic with blood flowing over the
 308 interdigitated gold electrical leads for 2 minutes with 3V applied electrical field before imaged for first instance of
 309 fibrin formation as visualized with fluorescently tagged fibrinogen. b. Comparison of control samples (no applied
 310 voltage) and 3V where there is statistical significance. c. Representative images of the control and 3V experiments
 311 showing that fibrin formed at 300secs in the applied voltage experiments, but did not appear until 480secs in the
 312 control. d. Peak temperature measured in the single channel gravity-driven microfluidic at applied voltages of 3-
 313 20V.

314

315 *In vivo* animal experiments

316 To test the efficacy of our device and overall premise on hemostasis *in vivo*, we utilized a
 317 well-established rat femoral vessel traumatic injury model^{26, 27, 28, 29} (Figure 4a). This model
 318 results in an easily visualized, continuous stream of blood flowing from the injury site. The
 319 devices used were made of interdigitated 0.1mm platinum wires anchored to a bandage. The

320 femoral vein was isolated *in situ* on the animal subjects. The vein was punctured with a 22-gauge
321 needle and allowed to bleed. Five different conditions (injury only, bandage, bandage+3V,
322 bandage+6V, and bandage+9V (applied microelectronic device)) were compared in terms of
323 bleeding time and the weight of blood lost. Bleeding time was recorded as the elapse time when
324 bleeding had ceased for a minimum of 10 seconds, an ANOVA and Tukey test were performed
325 and found statistical significance between injury only and bandage+9V conditions, as shown in
326 Figure 4b. Bandage+3V and bandage+6V did result in lower bleeding times as compared to the
327 injury only and bandage but were not significant. Additionally, the weight of blood lost was
328 measured in each subject over time, with the results shown in Figure 4c. The weight of blood lost
329 was collected with gauze applied under the wound and changed every 30 seconds. With applied
330 voltage (either 3, 6 or 9V) there was less blood loss (in terms of weight) when compared to both
331 injury only and bandage (gauze only). The arrows in Figure 3c indicate the point at which the
332 measured blood weight was constant, indicating that bleeding had stopped. In the injury only
333 experiments, the time at which the blood weight was constant varied between 150 and 480
334 seconds, which resulted in the noticeable slight increased slope (Figure 3c) and no single point
335 where the blood weight is constant. Throughout the experiments, no localized burns or gross side
336 effects were detected in the animals. Histology analysis of tissue with MSB staining (Figure 4d)
337 showed electrical stimulation led to increased fibrin formation at the injury site as compared to
338 control conditions as highlighted with the white dotted circles. Veins were shown to have more
339 fibrin formation (stained red) with bandage+9V than with injury only, suggesting that the applied
340 electric field enhances fibrin formation.



341

342 **Figure 4** – a. The electrical bandages were tested on rat femoral veins. b. Bleeding time was measured for injury
 343 only, bandage, bandage with 3V, bandage with 6V, and bandage with 9V where there was statistical significance
 344 between the injury only and bandage with 9V. c. The total weight of blood loss was measured over time between the
 345 injury only, bandage, bandage with 3V, bandage with 6V, and bandage with 9V, showing that the bandage with
 346 voltage (3, 6, or 9V) has less total blood loss as compared to injury only and bandage. d. MSB histological staining
 347 of injury only and bandage with 9V where fibrin is highlighted in white dotted circles and more fibrin is found in the
 348 bandage with 9V.

349

350 Blood clots are formed from two primary components: a fibrin mesh-network and
 351 platelets. The fibrin mesh-network is formed from the blood protein-fibrinogen and enhances the
 352 structural integrity of the clot, while cell fragments-platelets contract the clot to bring the injured
 353 blood vessel walls closer together in order to facilitate healing. Currently there are many
 354 hemostatic agents on the market that facilitate clotting including biologics and topical powders.

355 However, these agents all have drawbacks that prevent them from widespread use. Biologics
356 such as activated factor VII and fibrin glue are made from bovine and human components and
357 are therefore inappropriate for low-resource settings and carry risks of bloodborne infections and
358 immune dysregulation. Additionally, the application of pressure is a mainstay of hemostasis
359 treatments³⁰, but some injuries result in non-compressible hemorrhaging. Topical products are
360 ineffective for non-compressible hemorrhage, and can have local side effects such as burns,
361 contusions, and local over clotting. These issues highlight a need for a novel hemostatic agent
362 that can treat non-compressible hemorrhage in environments where traditional solutions are
363 impractical.

364 Here we have presented result showing that *in vitro* fibrin formation occurs within 300
365 seconds with 3V and *in vivo* hemostasis occurs under 150 seconds at 9V. There are obvious
366 differences and factors between the *in vitro* and *in vivo* conditions, such as the presence of tissue
367 factor, which will enhance the hemostatic response occurring *in vivo*. Therefore, our *in vitro*
368 results cannot be directly compared to *in vivo* results, but to our knowledge, these results are the
369 first presented using low voltage applied electric fields to achieve rapid hemostasis with in both
370 *in vitro* and *in vivo*. We investigated the addition of pressure with our *in vitro* microelectronic
371 device and found no improvement in clotting time or clot formation, as shown in Supplemental
372 Figure 3. Our microelectronic device did achieve rapid hemostasis independent of pressure, in
373 turn demonstrating the ability as a potential hemostatic agent for the treatment of non-
374 compressible hemorrhage.

375 Previously mentioned was the use of direct current (DC) in our microelectronic device.
376 There are two main types of electrical current: direct current (DC) and alternating current (AC).
377 DC refers to electrons flowing in one direction and is usually produced by a battery. AC

378 continuously switches direction, on/off, within a cycle (referred to as frequency), cellular ions
379 are able to depolarize and then repolarize. However, at high frequencies, switching occurs too
380 rapidly for depolarization/repolarization, so the electrical energy is converted directly to heat -
381 the main mechanism used in electrosurgery and electrocautery. In living tissue, current flow
382 consists of the transfer of charged ions within cells and the human body acts as a conductor for
383 electrical current due to the electrolyte composition of its cells. When applied to living tissue,
384 direct current depolarizes cell membranes and leads to neuromuscular excitation. If the voltage
385 and current is sustained for a long period of time, cell death can occur¹¹. Here we are using DC
386 provided by a power source to mimic power that would be provided by a simple 9V battery, in a
387 limited manner (low voltage and short period of constant time), resulting in depolarization of the
388 cells membranes without heat effects while achieving rapid hemostasis.

389 As was shown in Figure 1b, our microelectronic device design uses a 9V battery which
390 allows for mobile applications, simple operation, key features for injuries occurring in combat or
391 in medically underserved communities. Medically underserved communities are those defined
392 by too few or geographically distant medical clinics, within the US 20% of Americans live in
393 these areas³¹. Combat situation are another medically limited resource setting where serious
394 traumatic wounds involving heavy bleeding and hemorrhage injuries experienced by military
395 personal are difficult to treat. Incorporating our microelectronic device into a bandage, the
396 device provides the ability to close and cover the wound in one simple manner and achieve
397 hemostasis.

398 Previous research by Fridman¹² and Kalghati¹³ found that there was no significant change
399 in calcium ion concentration or change in pH concentration during the time of coagulation in
400 their e-plasma treated blood samples. Their conclusion indicated that the direct conversion of

401 fibrinogen into fibrin may be one of the mechanisms by which non-thermal e-plasma initiates
402 coagulation. Our research found that with a 3V electric field, there is a direct conversion of
403 fibrinogen into fibrin, as shown in Figure 3b and c, with minimal local heating across a range of
404 voltages 3-20V (Figure 3d). However, a limitation of our single channel microfluidic design is
405 the limited volume of blood under test. Voltages between 4-9V resulted in large bubbles in the
406 microfluidic channel, occluding the channel (not shown here). It is thought that the bubbles are
407 caused by irreversible cell depolarization and not thermal effects, as stated previously. Referring
408 back to Ohm's law where voltage is equal to current \times resistances, where resistances is the
409 resistance of the blood cells and is considered a constant value. As voltage increases, current
410 will increase resulting in cell depolarization and channel occlusion as described above. With
411 larger volumes (i.e. a larger resistance values) of blood this effect should not occur and in fact
412 did not occur during the *in vivo* animal studies shown in Figure 4.

413 During the *in vivo* animal experiments 3, 6, and 9V were tested as compared to controls
414 with no localized burns or gross side effects detected in the animals, therefore electrical thermal
415 heat is not the mechanism for the triggered coagulation. Histology of femoral veins exposed to
416 the DC electrical field device resulted in more fibrin formation as compared to control, leading to
417 the conclusion that the electrical field treatment presented here does have a direct effect on
418 fibrinogen into fibrin and faster coagulation time. Further research is needed to understand on a
419 cellular level how the electrical field interacts with fibrinogen and the direct conversion into
420 fibrin.

421 Herein, we presented results showing that the application of low voltage electrical
422 stimulation at an injury site promotes faster clot formation without excessive heating and
423 accelerates fibrin formation and hence, hemostasis overall. Specifically, our application found

424 fibrin formed 1.5x faster *in vitro*. *In vivo*, total cessation of bleeding was 2.5x faster, resulting in
425 2x less blood loss. This application of low voltage to sites of vascular injury represents an
426 entirely new and novel class of hemostatic agents that are electrically-based (wherein are free
427 from the infectious risks and immune effects that encumber current human or animal-derived
428 agents) and will have significant implications for experimental and clinical hematology.

429

430 CONCLUSION

431 We discovered that low voltage delivered by an interdigitated microelectronic device
432 incorporated into a simple bandage induces rapid hemostasis *in vitro* and *in*
433 *vivo* bleeding. Bleeding models demonstrate that blood in direct contact with the stimulated
434 electrical field induces faster clot formation without excessive heating or thermal tissue
435 destruction. Further investigation found low voltage, direct current electrical fields accelerate the
436 direct conversion of fibrinogen into fibrin and hemostasis overall. This represents a new
437 paradigm of hemostatic agents (free from infectious risks and immune effects of current human
438 or animal-derived agents) that are electrically-based but also leverage low voltage that
439 will have significant implications for clinical hematology, surgery, and trauma medicine.

440

441 AUTHOR CONTRIBUTIONS

442 ETH and WAL conceptualized the technology, planned and performed experiments, interpreted
443 data, and wrote the manuscript. YJW, SI, and YS performed the experiments and analyzed the
444 data. RGM completed the modeling shown in Figure 2. TC, YY, and HW completed the
445 modeling shown in Figure 1. THB and ACB completed the *in vivo* animal experiments and
446 edited the manuscript.

447

448 CONFLICT of INTEREST

449 There are no conflicts to declare.

450

451 DATA AVAILABILITY

452 The datasets generated during and/or analyzed during the current study are available from the
453 corresponding author on reasonable request.

454

455 ACKNOWLEDGEMENTS

456 This work was performed in part at the Georgia Tech Institute for Electronics and
457 Nanotechnology, a member of the National Nanotechnology Coordinated Infrastructure, which is
458 supported by the National Science Foundation (Grant ECCS-1542174).

459

460

461

462 REFERENCES

-
- 1 Reynolds, P.S., Michael, M.J., Cochran, E.D., Wegelin, J.A., Spiess, B.D., Prehospital Use of Plasma in Traumatic Hemorrhage (the PUPTH Trial): Study Protocol for a Randomized Controlled Trial. *Trials*, 16, 1693 (2015).
 - 2 Mitra, B., Cameron, P.A., Parr, M.J., Phillips, L., Recombinant Factor VIIa in Trauma Patients with the “Triad of Death.” *Injury* 43, 1409–1414 (2012).
 - 3 Singer, A.J., McClain, S.A., and Katz, A., A porcine epistaxis model: Hemostatic effects of octylcyanoacrylate, *Otolaryngol Head Neck Surg* 130, 553-7 (2004).
 - 4 Eaglstein W.H., Sullivan T.P., Giordano P.A., Miskin B.M., A liquid adhesive bandage for the treatment of minor cuts and abrasions. *Dermatol Surg.*, 28, 263-7 (2002).
 - 5 Bruns T.B. and Worthington, J.M., Using Tissue Adhesive for Wound Repair: A Practical Guide to Dermabond, *Am Fam Physician.*, 61(5), 1383-1388, (2000).
 - 6 Singer, A.J., McClain, S.A., and Katz, A., A porcine epistaxis model: Hemostatic effects of octylcyanoacrylate, *Otolaryngol Head Neck Surg* 130, 553-7 (2004).
 - 7 Eaglstein W.H., Sullivan T.P., Giordano P.A., Miskin B.M., A liquid adhesive bandage for the treatment of minor cuts and abrasions. *Dermatol Surg.*, 28, 263-7 (2002).
 - 8 Robinson, J.K., Hanke, C.W., Siegel, D., Fratial, A., Bhatia, A.C., Rohrer, T.E., *Surgery of Skin, Third Edition*, (Elsevier Inc., 2015).
 - 9 Bruns T.B. and Worthington, J.M., Using Tissue Adhesive for Wound Repair: A Practical Guide to Dermabond, *Am Fam Physician.*, 61(5), 1383-1388, (2000).
 - 10 Stover, J.H., “An electric defibrillator for cardiac resuscitation, *US Armed Forces Med J.*, 2(1), 57-61 (1951).
 - 11 Massarweh, N.N., Cosgriff, N., and Slakey, D.P., Electrosurgery: history, principles, and current and future uses. *J Am Coll Surg*, 202, 520 (2006).
 - 12 Fridman, G., et al., Blood coagulation and living tissue sterilization by floating electrode dielectric barrier discharge in air,” *Plasma Chem. Plasma Process.*, 26 (4), 425–442, (2006).
 - 13 Kalghatgi, S.U. et al., Mechanism of blood coagulation by nonthermal atmospheric pressure dielectric barrier discharge plasma, *IEEE Trans Plasma Sci*, 35, 1559-66 (2007).
 - 14 Mannino, R.G., Myers, D.R., Ahn B., Wang Y., Rollins, M., Gole, H., Lin, A.S, Guldberg R.E., Giddens, D.P., Timmins, L.H., and Lam, W.A. Do-it-yourself in vitro vasculature that recapitulates in vivo geometries for investigating endothelial-blood cell interactions. *Scientific reports*. 5, 12401 (2015).
 - 15 Gerwen, P.V., et al, Nanoscaled interdigitated electrode arrays for biochemical sensors, *Sens. and Actuators B*, 49, 73–80 (1998).
 - 16 MacKay, S., Hermansen, P., Wishart, D., Chen, J., Simulations of interdigitated electrode interactions with gold nanoparticles for impedance-based biosensing applications, *Sensors*, 15, 22192-22208 (2015).
 - 17 Igreja, R.,Dias, C.J., Analytical evaluation of the interdigital electrodes capacitance for a multi-layered structure, *Sens. Actuators A*, 112, 291–301 (2004).
 - 18 Hardy, E., Sakurai, Y., Sanjaya, N., Wolberg, A.S., and Lam, W.A., Effect of locally applied electricity on clot formation and hemostasis, *Blood*, 120, 2220 (2012).

-
- 19 O’Sullivan, C.T., Ohm’s law and the definition of resistance, *Phys. Educ.* 15, 237 (1980).
- 20 Fish, R.M. and Geddes, L.A., Conduction of electrical current to and through the human body: a review, *Eplasty*, 9, e44 (2009).
- 21 Nichols, A.B., Weiss, M.B., Sciacca, R.R., Cannon, P.J., and Blood, D.K., Relationship between segmental thallium-201 uptake and regional myocardial blood flow in patients with coronary artery disease, *Circulation* 68(2), 310-320 (1983).
- 22 Park, H., Yeom, E., Lee, S. J., X-ray PIV measurement of blood flow in deep vessels of a rat: An in vivo feasibility study. *Sci. Rep.* 6, 19194 (2016).
- 23 Jamison, R.A., Dubsky, S., Siu, K.K.W., Hourigan, K., and Fouras, A., X-ray velocimetry and haemodynamic forces within a stenosed femoral model at physiological flow rates, *Ann. Biomed. Eng.*, 39(6), 1643–1653 (2011).
- 24 Giangrande, P.L.F., Six characters in search of an author: the history of the nomenclature of coagulation factor, *Brit. J. Haematol.*, 121 (5), 703-717 (2003).
- 25 Fuss, C., Palmaz, J.C., and Sprague, E.A., Fibrinogen: Structure, Function, and Surface Interactions, *J Vasc Interv Radiol.*, 12, 677–682 (2001).
- 26 Bertram, JP., Williams, CA., Robinson, R., Segal, SS., Flynn, NT., and Lavik, EB., Intravenous hemostat: nanotechnology to halt bleeding. *Sci Transl Med*, 1, 11 (2009).
- 27 Fuglsang, J., Stender, M., Zhou, J., Moller, J., and Ravn, HB, Platelet activity and in vivo arterial thrombus formation in rats with mild hyperhomocysteinaemia, *Blood Coagulation & Fibrinolysis*, 13, 683 (2002).
- 28 Ersoy, G., Kaynak, M.F., Yilmaz, O., Rodoplu, U., Maltepe, F., and Gokmen, N. Hemostatic effects of Microporous Polysaccharide Hemosphere® in a rat model with severe femoral artery bleeding. *Adv Ther.* 24(3), 485–92 (2007).
- 29 Brown, A.C, Stabenfeldt, SE, Ahn, B., Hannan, RT, Dhada, KS, Herman, ES, Stefanelli, V., Guzzetta, N. Alexeev, A, Lam, W.A., Lyon, L.A., and Barker, T.H. Ultrasoft microgels displaying emergent platelet-like behaviours. *Nat. Mater.* 13 (12), 1108 (2014).
- 30 Gruen, R.L., Brohi, K, Schreiber, M., Balogh, Z. J., Pitt, V., Narayan, M., and Maier, R. V., Haemorrhage control in severely injured patients, *Lancet*, 380, 1099 (2012).
- 31 Bureau of Health Workforce. Designated Health Professional Shortage Areas Statistics. Health Resources and Services Administration (HRSA), U.S. Department of Health & Human Services (2016).

An interdigitated microelectronic device that applies low voltage (<9V) electrical field augments hemostasis *in vitro* and *in vivo*.

